Available online at www.sciencedirect.com
ScienceDirect
Journal of Sound and Vibration 306 (2007) 751–765
JOURNAL OF SOUND AND VIBRATION
www.elsevier.com/locate/jsvi

Generation of prescribed strain waves in an elastic bar by use of piezoelectric actuators driven by a linear power amplifier

A. Jansson*, U. Valdek, B. Lundberg

The Ångström Laboratory, Uppsala University, Box 534, SE-751 21 Uppsala, Sweden

Received 1 March 2007; received in revised form 22 May 2007; accepted 20 June 2007
Available online 10 August 2007

Abstract

The problem of generating prescribed strain waves in an elastic bar by means of a pair of piezoelectric actuators driven in phase by a linear power amplifier was considered theoretically and experimentally. The power amplifier was characterized by its DC voltage gain and 3 dB cut-off frequency unloaded, and by its output resistance and inductance. With the assumption of one-dimensional (1D) wave propagation in the bar, including the actuator region, a linear difference equation was derived for the required input voltage to the power amplifier in terms of the strain associated with the prescribed wave. This difference equation was solved numerically for a bell-shaped strain wave and for a single-period sine strain wave. After identification of the linear power amplifier, two tests were carried out with the aim to generate the two strain waves in an aluminium bar instrumented with semi-conductor strain gauges. Very good agreement was obtained between the implemented and required input voltages, output voltages and output currents of the power amplifier, and good agreement was achieved between the implemented and prescribed strain waves.

1. Introduction

Piezoelectric elements in the form of thin plates are increasingly used as sensors (e.g. Refs. [1,2]), and actuators (e.g. Refs. [3,4]), in structural, space, medical and other applications. This is largely explained by their ability of giving electrical response when subjected to mechanical stimuli, and vice versa, as described by two coupled constitutive equations [5], the actuator equation and the sensor equation, that relate the mechanical and electrical fields in the piezoelectric material. Plate-shaped piezoelectric elements also have large bandwidth, and they are suitable for integration into structures.

Studies of the interaction of piezoelectric actuators, driven by linear power amplifiers, and host structures generally involve consideration of the two constitutive equations, the dynamics of the amplifier and associated electric circuits, the dynamics of the actuator, and the dynamics of the host structure. Sometimes, however, one or several of these considerations can be left out. In particular, the sensor equation and the dynamics of the amplifier can be neglected if the actuators are driven by an amplifier with sufficiently low output impedance and large bandwidth. Furthermore, the actuator may be considered quasi-static if it is sufficiently

*Corresponding author.
E-mail address: anders.jansson@angstrom.uu.se (A. Jansson).

0022-460X/$ - see front matter
doi:10.1016/j.jsv.2007.06.013

Nomenclature

Latin

a	distance between bar cross-sections 0 and 1
A	cross-sectional area
c	wave speed
C	capacitance
d	piezoelectric constant
e	strain
E	Young's modulus
f	frequency
F	frequency-dependent part of transfer function K
G	voltage gain of amplifier
h	height
i	current
k	square root of piezoelectric coupling coefficient
K	transfer function, voltage to strain
l	length
L	inductance
R	resistance
t	time
U	voltage
w	width
x	axial coordinate
y	transverse coordinate (horizontal)
z	transverse coordinate (vertical)
Z	impedance, characteristic impedance

Greek letters

ε	permittivity
θ	Heaviside unit step function
ν	Poisson's ratio
ρ	density
ω	angular frequency

Superscripts

0	ideal amplifier
E	electrical
imp	implemented
M	mechanical
pre	prescribed
req	required

Subscripts

0	actuator region; cross-section at actuator/bar interface
1	bar cross-section at which strain is measured
a	actuator
ax	axial
b	bending
c	core
cut	cut-off (3 dB reduction)
em	electromagnetic
L	loaded amplifier
out	amplifier output
tr	transverse

small. Such simplifications were made, e.g., in the early work by Crawly and de Luis [6] on the interaction of piezoelectric actuators and an Euler–Bernoulli beam.

The dynamics of the actuator was taken into account, e.g., by Pan et al. [7], who studied an Euler–Bernoulli beam with attached piezoelectric actuators. Allowance for the interaction of host structure and electrical circuits, and for the two coupled constitutive equations was made, e.g., by Hagood et al. [8], Thornburgh and Chattopadhyay [9], and Thornburgh et al. [10]. Similar considerations were made also in studies of passive electrical damping systems [11]. Studies of power requirements, with consideration of the dynamics of the amplifier, were carried out, e.g., by Niezrecki and Cudney [12] and Leo [13].

A theoretical basis for generation of extensional waves in a linearly viscoelastic bar with a pair of piezoelectric actuators driven in phase by a linear power amplifier was developed in a preceding paper by the authors [14]. Allowance was made for the two constitutive equations, the dynamics of the amplifier, the dynamics of the actuator, and the dynamics of the bar. The problems of finding (i) the wave output produced by a given voltage input to the amplifier and (ii) the voltage input to the amplifier required to generate a desired wave output were considered, both in the frequency domain. In control applications involving waves, the second of these problem is particularly important as waves prescribed on the basis of sensor data can be used to cancel unwanted waves. Such cancellation is the basis, e.g., for the concept of a "mechanical wave diode", which uses feed-forward control in order to achieve one-way transmission of waves in an elastic bar [15].

In this paper, the problem of generating prescribed strain waves in an elastic bar with a pair of piezoelectric actuators driven in phase by a linear power amplifier is considered theoretically and experimentally. In Section 2, the theoretical results of Jansson and Lundberg [14] are adapted to a case involving an elastic bar and a power amplifier characterized by its DC voltage gain and 3 dB cut-off frequency unloaded, and by its output resistance and inductance. It is shown that in this case, the problem of generating prescribed strain waves can be solved in the time domain. In this way, difficulties at frequency zero can be avoided for prescribed strain waves with non-zero DC component. In Section 3, the procedures are described for identification of a linear power amplifier and experimental implementation of two prescribed strain waves, one with and one without a DC component, in an aluminium bar. In Section 4, theoretical results for the required input voltage to the amplifier, the required output voltage and output current from the amplifier and the prescribed strain in the bar are compared with corresponding results from the experimental implementation. Conclusions are summarized in Section 5.

2. Theoretical basis

2.1. Model of the electromechanical system

Consider the electromechanical system in Fig. 1 consisting of a long elastic bar with a pair of attached piezoelectric actuators driven in phase by a linear power amplifier.

The length of the actuator region $-x_0<x<x_0$ is $l_0=2x_0$, where x is an axial coordinate as shown. Thin bonding layers are assumed to have the only effect of perfectly attaching the actuators to the bar. The cross-sections of the bar and the actuators are rectangular, and the full cross-sections are symmetric with respect to the y- and z-axis. Outside the actuator region, the bar has height h, width w and cross-sectional area $A=hw$. In the core of the actuator region, it has height h_c, width w_c and cross-sectional area $A_c=h_cw_c$. Each actuator has height h_a, width w_a and cross-sectional area $A_a=h_aw_a$. Therefore, the total cross-sectional area is $A_0=2A_a+A_c$ within the actuator region.

The Young's modulus of the bar material is assumed to be E, while that of the actuators, when short-circuited, is assumed to be E_a. Further, it is assumed that initially plane cross-sections remain plane and that the stress is uni-axial in the x direction. Therefore, the effective Young's modulus is $E_0=(2A_aE_a+A_cE)/A_0$ within the actuator region. Similarly, the densities are assumed to be ρ and ρ_a, respectively, and therefore the effective density is $\rho_0=(2A_a\rho_a+A_c\rho)/A_0$ within this region. The wave speeds in the bar and actuator regions are $c=(E/\rho)^{1/2}$ and $c_0=(E_0/\rho_0)^{1/2}$, respectively, while the characteristic impedances in these regions are $Z^M=AE/c$ and $Z_0^M=A_0E_0/c_0$, respectively.

The piezoelectric material is assumed to be polarized in the z direction and to have a linear electromechanical response. In addition to the short-circuited Young's modulus E_a, this response is characterized by the permittivity ε_a and piezoelectric constant $d_a=-d_{31}$. The electrical fields between the conducting layers on the upper and lower faces of the actuators are assumed to be parallel to the z-axis, and the effects of strains in the y and z directions are neglected.

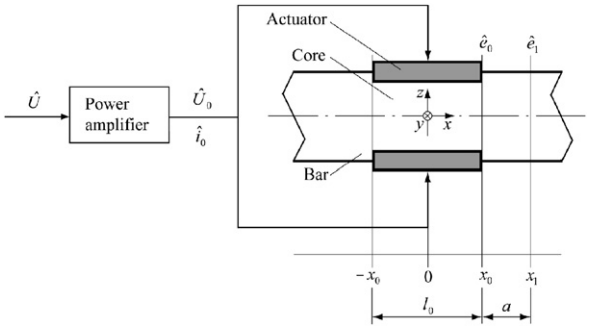

Fig. 1. Electromechanical system consisting of linear power amplifier, piezoelectric actuators and bar.

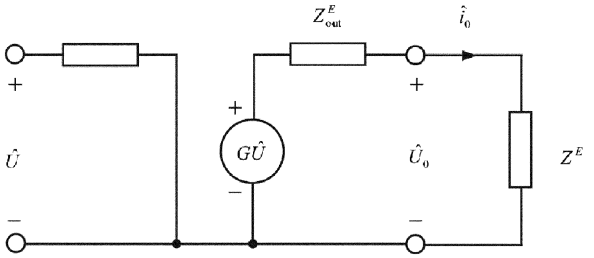

Fig. 2. Equivalent circuit of linear power amplifier driving actuator–bar assembly. The voltage gain of the unloaded amplifier is $G(\omega)$ and its output impedance is $Z^E_{\text{out}}(\omega)$. The load impedance provided by the actuator–bar assembly is $Z^E(\omega)$.

The actuators are driven in parallel and in phase by a linear power amplifier as shown in Fig. 2. The amplifier is characterized by its voltage gain $G(\omega)$ unloaded and its output impedance $Z^E_{\text{out}}(\omega)$. The electrical impedance of the loading actuator–bar assembly is $Z^E(\omega)$. As a result of the mechanical response of the actuators, strain waves are generated which propagate symmetrically in opposite directions through the bar, away from the actuator region. The associated strain $\hat{e}_1(\omega) = \hat{e}(x_1, \omega)$ is measured at a distance $a = x_1 - x_0$ from the interface $x = x_0$, where the strain is $\hat{e}_0(\omega) = \hat{e}(x_0, \omega)$.

2.2. Dynamics of the electromechanical system

The output voltage $\hat{U}_0(\omega)$ and the output current $\hat{i}_0(\omega)$ of the amplifier can be expressed in terms of the input voltage $\hat{U}(\omega)$ as

$$\hat{U}_0 = G_L \hat{U}, \quad \hat{i}_0 = \frac{\hat{U}_0}{Z^E}, \tag{1a,b}$$

where

$$G_L = \frac{Z^E}{Z^E + Z^E_{\text{out}}} G \tag{2}$$

is the voltage gain of the amplifier loaded by the electrical impedance of the actuator–bar assembly. This impedance is [14]

$$Z^E = \frac{Z^E_0}{1 - k^2(1 - 4F^0 Z^M_a / Z^M)}, \tag{3}$$

where the function $F^0(\omega)$ is given by

$$F^0 = \frac{\mathrm{e}^{\mathrm{i}\omega x_0/c_0} - \mathrm{e}^{-\mathrm{i}\omega x_0/c_o}}{p^0 \mathrm{e}^{\mathrm{i}\omega x_0/c_0} - q^0 \mathrm{e}^{-\mathrm{i}\omega x_0/c_0}} \tag{4}$$

with

$$p^0 = 1 + \frac{Z^M_0}{Z^M}, \quad q^0 = 1 - \frac{Z^M_0}{Z^M}. \tag{5}$$

Here $k^2 = d_a^2 E_a/\varepsilon_a$ is the piezoelectric coupling coefficient [5]. The quantity $Z^E_0 = Z^E_a/2$ is the electrical impedance of the two actuators, electrically in parallel and mechanically unloaded, $Z^E_a(\omega) = 1/\mathrm{i}\omega C_a$ is the electrical impedance of a single mechanically unloaded actuator with capacitance $C_a = \varepsilon_a l_0 w_a / h_a$. The quantity $Z^M_a = A_a E_a / \mathrm{i}\omega l_0$ is the mechanical impedance of a single short-circuited actuator with one end fixed and the other end loaded quasi-statically in the axial direction.

The strains $\hat{e}_1(\omega)$ and $\hat{e}_0(\omega)$ are related to each other and to the input voltage $\hat{U}(\omega)$ of the amplifier through the relations

$$\hat{e}_1 = \hat{e}_0 \mathrm{e}^{-\mathrm{i}\omega a/c}, \tag{6}$$

$$\hat{e}_0 = K_L G_L \hat{U}. \tag{7}$$

The transfer function $K_L(\omega)$, from the output voltage $\hat{U}_0$ of the amplifier to the strain $\hat{e}_0$ in the bar at the end of the actuator region, is given by [14]

$$K_L = 2\frac{A_a E_a}{AE}\frac{d_a}{h_a}F^0. \tag{8}$$

From Eqs. (4) and (5) it follows that $K_L(0) = 0$, which means that it is not straight forward to solve the inverse problem of (6) and (7) in the frequency domain. Therefore, the gain of the unloaded amplifier and the output impedance of the amplifier are expressed parametrically as

$$G = \frac{G^0}{1 + \mathrm{i}\omega/\omega_{\mathrm{cut}}}, \quad Z^E_{\mathrm{out}} = R + \mathrm{i}\omega L, \tag{9}$$

which makes it possible to transform Eqs. (6) and (7) into the time domain. Here G^0 is the DC gain of the unloaded amplifier, $\omega_{\mathrm{cut}} = 2\pi f_{\mathrm{cut}}$ is the cut-off angular frequency at which $|G(\omega)|$ is 3 dB below its low-frequency limit G^0, R is the output resistance and L is the output inductance. With this parametric representation of the amplifier, Eqs. (2)–(8) and inversion of the Fourier transforms, give

$$e_1(t) = e_0(t - a/c), \tag{10}$$

$$\begin{aligned} U(t) = U(t - t_0) + \frac{1}{2}\frac{1}{G^0}\frac{h_a}{d_a}\frac{AE}{A_a E_a}\Bigg[& p^0 e_0(t) - q^0 e_0(t - t_0) + 8k^2 RC_a \frac{A_a E_a}{l_0 Z^M}(e_0(t) - e_0(t - t_0)) \\ & + (1/\omega_{\mathrm{cut}} + 2(1 - k^2)RC_a)\left(p^0 \frac{\mathrm{d}e_0}{\mathrm{d}t}(t) - q^0 \frac{\mathrm{d}e_0}{\mathrm{d}t}(t - t_0)\right) \\ & + 8k^2(RC_a/\omega_{\mathrm{cut}} + LC_a)\frac{A_a E_a}{l_0 Z^M}\left(\frac{\mathrm{d}e_0}{\mathrm{d}t}(t) - \frac{\mathrm{d}e_0}{\mathrm{d}t}(t - t_0)\right) \\ & + 2(1 - k^2)(RC_a/\omega_{\mathrm{cut}} + LC_a)\left(p^0 \frac{\mathrm{d}^2 e_0}{\mathrm{d}t^2}(t) - q^0 \frac{\mathrm{d}^2 e_0}{\mathrm{d}t^2}(t - t_0)\right) \\ & + 8k^2(LC_a/\omega_{\mathrm{cut}})\frac{A_a E_a}{l_0 Z^M}\left(\frac{\mathrm{d}^2 e_0}{\mathrm{d}t^2}(t) - \frac{\mathrm{d}^2 e_0}{\mathrm{d}t^2}(t - t_0)\right) \\ & + 2(1 - k^2)(LC_a/\omega_{\mathrm{cut}})\left(p^0 \frac{\mathrm{d}^3 e_0}{\mathrm{d}t^3}(t) - q^0 \frac{\mathrm{d}^3 e_0}{\mathrm{d}t^3}(t - t_0)\right)\Bigg], \end{aligned} \tag{11}$$

where $t_0 = l_0/c_0$ is the transit time for a wave through the actuator region. Thus, the problem of finding the required input voltage $U(t)$ for a prescribed strain $e_0(t)$ becomes a linear difference equation, while the inverse problem of finding the strain $e_0(t)$ produced by a given input voltage $U(t)$ becomes a linear third-order difference-differential equation.

For a wave defined by a prescribed strain pulse $e_0(t)$, the difference equation (11) can be solved for the required input voltage $U(t)$ to the amplifier in successive intervals of length t_0. This was done numerically for two different strain waves. The first wave was defined by the bell-shaped strain pulse

$$e_0 = e_{0\max}\sin^2(\pi t/2t_0)[\theta(t) - \theta(t - 2t_0)] \tag{12}$$

with amplitude $e_{0\max}$ and duration $2t_0$, and the second wave was defined by the single-period sine strain pulse

$$e_0 = e_{0\max}\sin(\pi t/2t_0)[\theta(t) - \theta(t - 4t_0)] \tag{13}$$

with amplitude $e_{0\max}$ and duration $4t_0$, where $\theta(t)$ is the Heaviside unit step function. Both waves are also defined by the delayed strain pulse $e_1(t)$ according to Eq. (10). The normalized strain pulses (12) and (13) and their normalized spectra are shown in Figs. 3 and 4, respectively, where time is normalized to t_0 and frequency to $f_0 = 1/t_0$. With the required input voltages $U(t)$ to the amplifier known, the corresponding output voltages $U_0(t)$ and output currents $i_0(t)$ were determined from Eqs. (1)–(5) and (9) by use of the discrete Fourier transform.

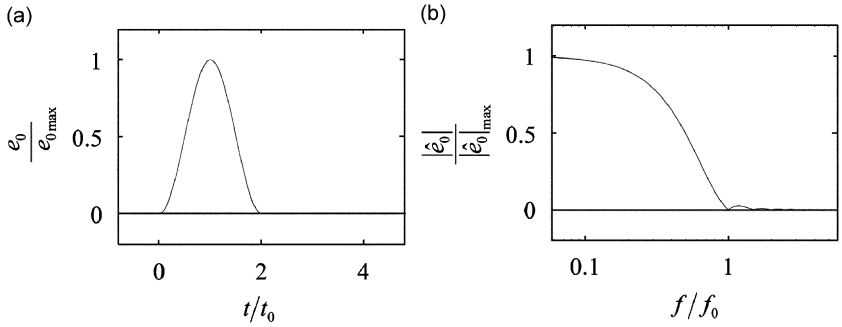

Fig. 3. (a) Prescribed bell-shaped strain pulse and (b) its spectrum.

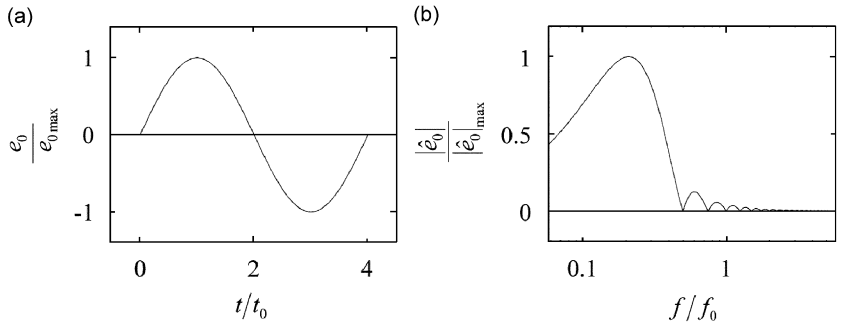

Fig. 4. (a) Prescribed single-period sine strain pulse and (b) its spectrum.

The following section presents the implementation of the strain pulses (12) and (13) experimentally. Then, in Section 4, comparisons will be made between the implemented and required results for the input voltage $U(t)$, the output voltage $U_0(t)$ and the output current $i_0(t)$, and between the implemented and prescribed strains $e_1(t)$.

3. Experimental tests

3.1. Identification of the linear power amplifier

A linear power amplifier (EPA-104, Piezo Systems, Inc.) was used to drive the actuators. This amplifier has an output current constraint of 200 mA. Therefore its response is linear only if the input voltage and the load impedance are such that the output current is within this constraint. The DC voltage gain of the unloaded amplifier was continuously variable from zero to 20. In all identification and wave generation tests the gain control was kept in the same position corresponding to a gain of approximately 12. The input voltage to the amplifier was provided by a signal generation card (DAQ-2010, Adlink Technology, Inc.).

Within its linear range, the power amplifier is characterized by its voltage gain unloaded $G(\omega)$, and its output impedance $Z^E_{\text{out}}(\omega)$ as illustrated in Fig. 2. These complex-valued functions of frequency were identified non-parametrically as follows. The amplifier was loaded with each of a series of 10 precision resistors (MP 930, Caddock Electronics, Inc.) with resistances 10, 20, 30, 40, 50, 75, 100, 150, 200 and 300 Ω. For each such load, the amplifier was subjected to a transient input voltage $U(t)$ taken as an approximately rectangular pulse with duration 8 μs. In each of these tests, the amplitude of the input voltage was chosen so that the output current of the amplifier would not exceed the 200 mA limit. The output voltage was reduced by a factor of 21 in a voltage divider consisting of two precision resistors (MP 925, Caddock Electronics, Inc.) with resistances 5 and 100 kΩ. The input voltage and the reduced output voltage were recorded by use of a digital oscilloscope card (UF.3122, Strategic Test Scandinavia AB). The sampling rate was 10 MHz, and no filter was used. All identification tests were carried out at room temperature.

With $Z^E(\omega)$ replaced by R_n in Fig. 2, the output current $\hat{i}_0$ can be expressed in two ways as $\hat{U}_0/R_n = G\hat{U}/(Z^E_{\text{out}} + R_n)$. For each discrete frequency ω, this leads to the over-determined linear system of 10 equations

$$(\hat{U}/\hat{U}_0)_n G - (1/R_n)Z^E_{\text{out}} = 1, \quad n = 1, 2, \ldots, 10 \tag{14}$$

for the two unknowns $G(\omega)$ and $Z^E_{\text{out}}(\omega)$. This system can be written as $\mathbf{Bp} = \mathbf{b}$, where $\mathbf{B}$ is a 10×2 matrix, $\mathbf{p}$ is a 2×1 column vector with the two unknowns as elements, and $\mathbf{b}$ is a 10×1 column vector with each element equal to one. The best solution of this system in the sense of least squares gives the non-parametric estimation of $G(\omega)$ and $Z^E_{\text{out}}(\omega)$. It is obtained as $\mathbf{p}_{\text{LS}} = \mathbf{B}^+\mathbf{b}$, where $\mathbf{B}^+ = (\mathbf{B}^*\mathbf{B})^{-1}\mathbf{B}^*$ is the Moore–Penrose pseudo-inverse matrix and $\mathbf{B}^* = \bar{\mathbf{B}}^{\text{T}}$ is the adjoint (conjugate and transpose) matrix of $\mathbf{B}$. The normalized error is defined as $\xi = \mathbf{r}^*\mathbf{r}/\mathbf{b}^*\mathbf{b}$ with $\mathbf{r} = \mathbf{Bp}_{\text{LS}} - \mathbf{b}$.

The parameters G^0, $\omega_{\text{cut}} = 2\pi f_{\text{cut}}$, R and L of the power amplifier model defined by Eq. (9) were estimated from the non-parametric results for $G(\omega)$ and $Z^E_{\text{out}}(\omega)$. The DC gain of the unloaded amplifier G^0 was estimated by averaging $\text{Re}[G(\omega)]$ in the interval [0,10] kHz of low frequencies. The cut-off frequency ω_{cut} was obtained from $|G(\omega_{\text{cut}})| = G^0/\sqrt{2}$. The resistance R and the inductance L were estimated by using the method of least squares in the frequency interval [10,100] kHz. The estimated parameters were used in the wave generation tests.

3.2. Generation of prescribed strain waves

The experimental set-up used for generation of prescribed strain waves is shown in Fig. 5.

An aluminium bar with length 2.80 m, height $h = 4.0$ mm and width $w = 4.0$ mm was used. Within the actuator region, the bar was milled symmetrically from two opposite sides over the length 95.4 mm to height $h_c = 1.02$ mm, while its width $w_c = 4.0$ mm was left the same as in the rest of the bar. The material of the bar had Young's modulus $E = 69$ GPa, Poisson's ratio $\nu = 0.30$ and density $\rho = 2700\,\text{kg/m}^3$.

In each milled slot, three piezoelectric plates (Piezo Systems, Inc., T226-A4-203Y, ceramic type 5A4E) with length 31.8 mm, height $h_a = 0.66$ mm and $w_a = 6.4$ mm were bonded in mechanical contact with each other, and connected electrically in parallel, so that they formed a compound actuator with length $l_0 = 95.4$ mm. The piezoelectric material of the plates had short-circuited Young's modulus $E_a = 66$ GPa, density $7800\,\text{kg/m}^3$, piezoelectric constant $d_{31} = -190 \times 10^{-12}$ m/V and permittivity $\varepsilon_a = 1.6 \times 10^{-8}$ A s/V m.

The dimensions and material properties of the actuator–bar assembly correspond to parameters as follows. The wave speed was $c = 5050$ m/s in the bar and $c_0 = 3300$ m/s in the actuator region. The transit time for a wave through the actuator region was $t_0 = 28.9\,\mu$s, and its inverse, corresponding to the number of transits per

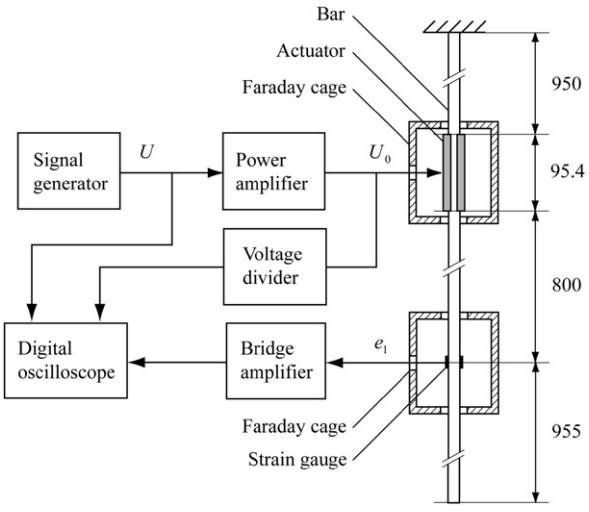

Fig. 5. Experimental set-up for generation of prescribed strain waves. Lengths in mm.

unit time, was $f_0 = 34.6\,\text{kHz}$. The characteristic impedance was $Z^M = 219\,\text{N s/m}$ in the bar and $Z_0^M = 254\,\text{N s/m}$ in the actuator region. The capacitance of an unloaded compound actuator was $C_a = 14.7\,\text{nF}$, and the piezoelectric coupling coefficient was $k^2 = 0.150$.

The bar was kept vertical, clamped at its upper end at a distance of 950 mm from the upper end of the actuator region and free at its lower end. In the lower part of the bar, at a distance of $a = 800\,\text{mm}$ from the lower end of the actuator region, the bar was instrumented with three semi-conductor strain gauges (Kyowa, type KSP-2-120-E3), viz., two with axial orientation opposite to each other and one with transverse orientation. The relatively large distance from the actuator region to the instrumented section of the bar was chosen in order to reduce the electromagnetic noise from the actuators picked up by the strain gauges. For the same reason, the actuators and the strain gauges were surrounded by Faraday cages, grounded together with the bar.

The two compound actuators, electrically in parallel, were driven by the linear power amplifier with input from the signal generation card. Each strain gauge was connected to a bridge amplifier (Vishay Measurements Group, 2210) with bandwidth 100 kHz (3 dB). Before the arrival of reflected waves from the ends of the bar, the input and output voltages $U(t)$ and $U_0(t)$ of the power amplifier, the axial strains $e'_{\text{ax}}(t)$ and $e''_{\text{ax}}(t)$, and the transverse strain $e_{\text{tr}}(t)$ were recorded by means of the digital oscilloscope card. No filters were used, and the sampling rate was 10 MHz.

In spite of the measures taken, each of the three measured strains was contaminated with electromagnetic noise from the pulse generation. However, a favourable angular orientation of the bar around its axis turned out to be such that none of the three strain gauges faced the closest wall of the Faraday cage. With this orientation of the bar the electromagnetic noise e_{em} was minimized and equalized, i.e., it was the same for each measured strain. Furthermore, contributions from accidental bending $\pm e_b$ to the measured axial strains had the same magnitude but opposite signs. Under these conditions, the three measured strains can be expressed as $e'_{\text{ax}} = e_1 + e_{\text{em}} + e_b$, $e''_{\text{ax}} = e_1 + e_{\text{em}} - e_b$, and $e_{\text{tr}} = -\nu e_1 + e_{\text{em}}$, where ν is Poisson's ratio. Therefore, with suppression of the contributions from both electromagnetic noise and bending, the strain $e_1(t)$ can be evaluated numerically from the expressions

$$e_1 = \frac{e_{\text{ax}} - e_{\text{tr}}}{1+\nu}, \quad e_{\text{ax}} = \frac{e'_{\text{ax}} + e''_{\text{ax}}}{2}. \tag{15}$$

For both the bell-shaped strain wave and the single-period sine strain wave, the implemented output current $i_0(t)$ was obtained numerically from the implemented output voltage $U_0(t)$, which was recorded, and by use of Eqs. (1b), (3)–(5), and a second-order Butterworth filter with cut-off frequency 100 kHz. Thus, the implemented output current is based on both measurement, theory and filtering. For the single-period sine strain wave, the same filter was used also for the required output current.

Two tests were carried out at room temperature with the aim to produce the waves defined by the prescribed bell-shaped strain pulse (Eq. (12)), with amplitude $e_{0\max} = 7\,\mu$ and duration $2t_0 = 57.8\,\mu\text{s}$ and the single-period sine strain pulse (Eq. (13)), with amplitude $e_{0\max} = 5\,\mu$ and duration $4t_0 = 115.6\,\mu\text{s}$.

4. Results and discussion

Figs. 3 and 4 show that the spectra of the prescribed strain pulses $e_0(t)$ are significant only below the approximate frequency $f \approx 35\,\text{kHz}$. At this frequency, the wave length in the aluminium bar is $\lambda = c/f \approx 0.14\,\text{m}$. This wave length is much larger than the transverse dimension 4 mm of the bar, and therefore the one-dimensional (1D) model used for the actuator–bar assembly can be expected to be valid [16].

The results of the identification of the linear power amplifier are shown in Fig. 6. The DC gain of the unloaded amplifier and the 3 dB cut-off frequency were estimated to be $G^0 = 12.1$ and $f_{\text{cut}} = 82\,\text{kHz}$, respectively. For the magnitude of the gain G of the unloaded amplifier, the parametric and non-parametric results are very close up to more than 100 kHz. However, the parametric results for the real and imaginary parts of this gain are somewhat higher and lower in magnitude, respectively, than the corresponding non-parametric results. The output resistance and the output inductance of the amplifier were estimated to be $R = 8.1\,\Omega$ and $L = 2.4\,\mu\text{H}$, respectively. For both the real and the imaginary parts of the output impedance Z^E_{out}, the parametric and non-parametric results are quite close up to more than 100 kHz, which suffices here.

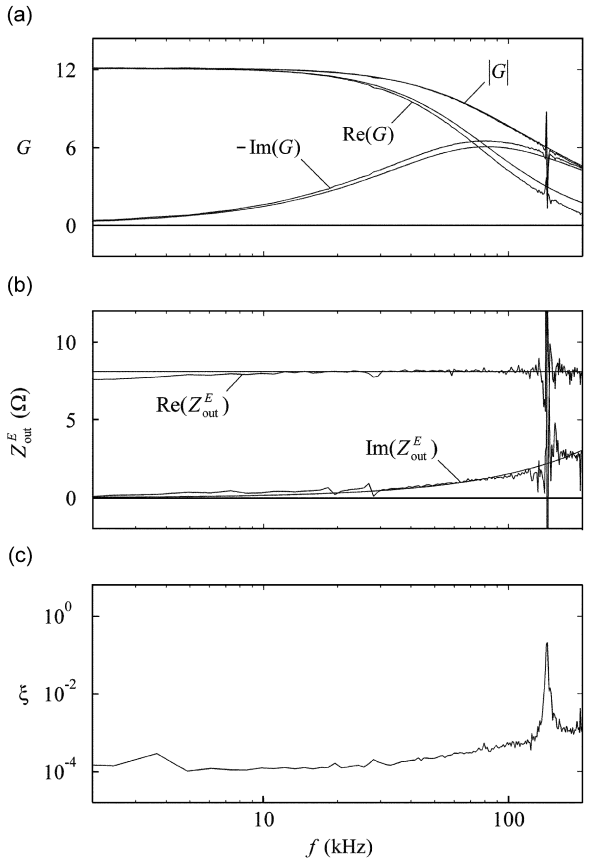

Fig. 6. (a) Voltage gain G, (b) output impedance Z^E_{out} and (c) minimized error ξ versus frequency f. Non-parametric (irregular curves) and parametric (smooth curves) results.

At higher frequencies, the non-parametric results become irregular. The reason is that the Fourier transform $\hat{U}(\omega)$ of the rectangular input pulse $U(t)$ to the amplifier is zero at frequencies that are integral multiples of the inverse of the pulse width 8 μs. Therefore, the excitation in the identification tests was weak or non-existent at and around 125 kHz. By reducing the pulse width further, e.g., to 5 μs, one can move the lowest problematic frequency up to 200 kHz, which is far outside the frequency interval of interest.

The ratio $G^L/G = Z^E/(Z^E + Z^E_{\text{out}})$ of the gain of the loaded amplifier to that of the unloaded amplifier versus frequency f is shown in Fig. 7. This result shows the effect of the output impedance $Z^E_{\text{out}} = R + \mathrm{i}\omega L$ on the gain of the amplifier subjected to the load Z^E of the actuator–bar assembly. The frequency dependence of the gain ratio is explained by the inductive nature of the output impedance and the capacitive nature of the load impedance which make $|Z^E + Z^E_{\text{out}}| < |Z^E|$. The result shows that the magnitude $|G^L/G|$, which is equal to one at low frequencies, has increased to 1.002 at 40 kHz and to 1.016 at 100 kHz. At these frequencies, the magnitude $|G|$ of the (parametric) gain of the unloaded amplifier has decreased to 0.90 and 0.63, respectively, of its value G^0 at low frequencies. This shows that for the amplifier used the effect of finite cut-off frequency is significantly larger than that of finite output impedance. For frequencies below 20 kHz, an ideal amplifier model with constant gain $G = G^0$ and zero output impedance $Z^E_{\text{out}} = 0$ would be quite accurate. Under such conditions $\omega_{\text{cut}} = \infty$, $R = 0$ and $L = 0$, and therefore all that remains on the right-hand side of Eq. (11) are the first three terms. Under the additional condition of matched impedances, $Z^M_0 = Z^M$, Eq. (5) give $p^0 = 2$ and $q^0 = 0$, and Eq. (11) is further reduced to

$$U(t) = U(t - t_0) + \frac{1}{G^0}\frac{h_a}{d_a}\frac{AE}{A_a E_a}e_0(t). \tag{16}$$

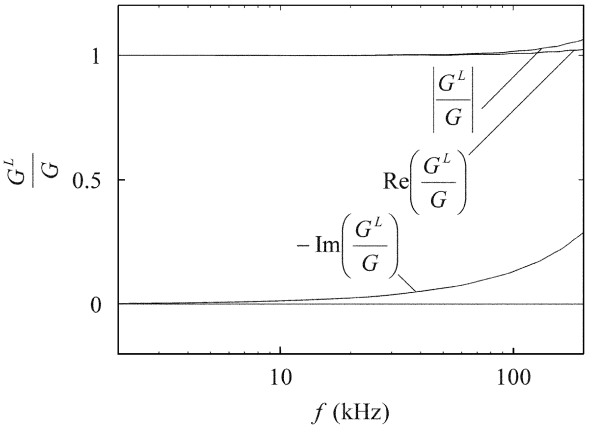

Fig. 7. Ratio G^L/G of the gain of the loaded amplifier to that of the unloaded amplifier versus frequency f.

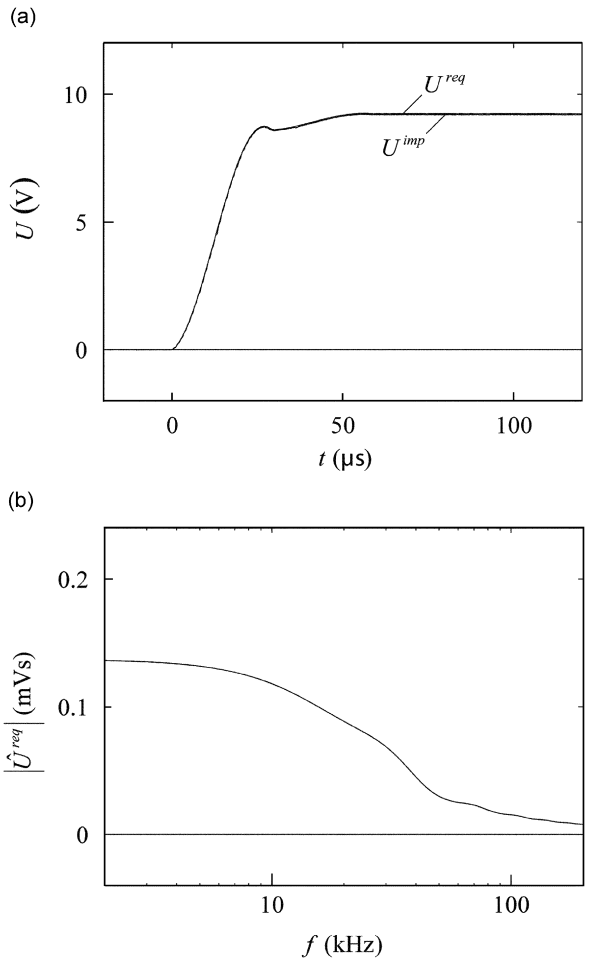

Fig. 8. Generation of bell-shaped strain wave: (a) required and implemented input voltages U versus time t; and (b) spectrum of required input voltage.

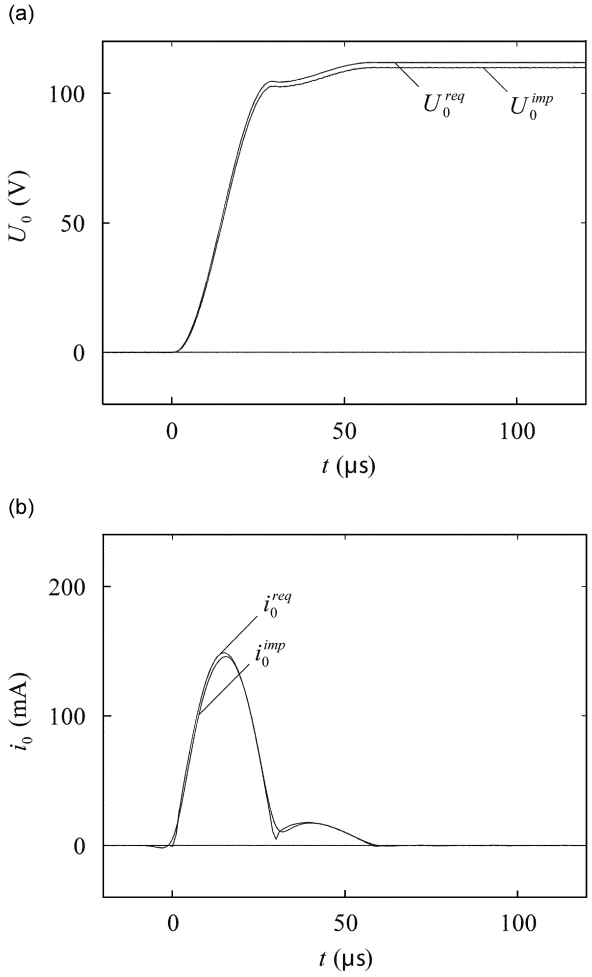

Fig. 9. Generation of bell-shaped strain wave. Required and implemented (a) output voltage U_0 and (b) output current i_0 versus time t.

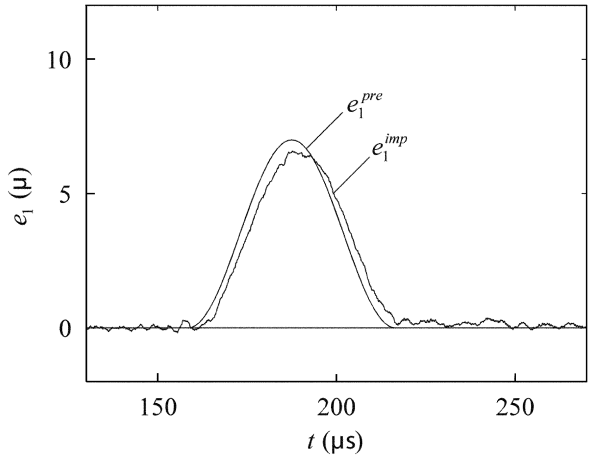

Fig. 10. Generation of bell-shaped strain wave. Prescribed and implemented strain e_1 versus time t.

Because of its simplicity, such a model may be advantageous in control applications where high computational speed is of primary importance. However, the full Eq. (11) was used to produce the results which follow.

The results obtained for generation of the bell-shaped strain wave of Fig. 3 are shown in Figs. 8–10. The required and implemented input voltages U versus time t, and the spectrum of the required input voltage, are shown in Fig. 8. The implemented voltage is very close to that required. The spectrum is significant up to more than 100 kHz, which means that the output impedance of the amplifier has a certain influence. The required and implemented output voltages U_0 and output currents i_0 are shown versus time t in Fig. 9. The implemented voltage and current are very close to those required. The maximum output current is well below the current limit of 200 mA, which means that the amplifier operated within its linear range. All changes in the input voltage, the output voltage, and the output current occur in a time approximately equal to the duration $2t_0 \approx 58\,\mu s$ of the prescribed strain pulse. The prescribed and implemented strains e_1 are shown versus time t in Fig. 10. As shown by Eq. (10), this prescribed strain is just a delayed version of the prescribed strain e_0. Even though the implemented strain is only about 7 μ, it is seen to be insignificantly disturbed by noise, and the agreement with the prescribed strain is good. Without the considerations and measures behind Eqs. (15), however, the level of electromagnetic noise was about 2 μ, i.e., it was quite comparable to that of the signal.

The results obtained for generation of the single-period sine strain wave of Fig. 4 are shown in Figs. 11–13. The required and implemented input voltages U versus time t, and the spectrum of the required input voltage,

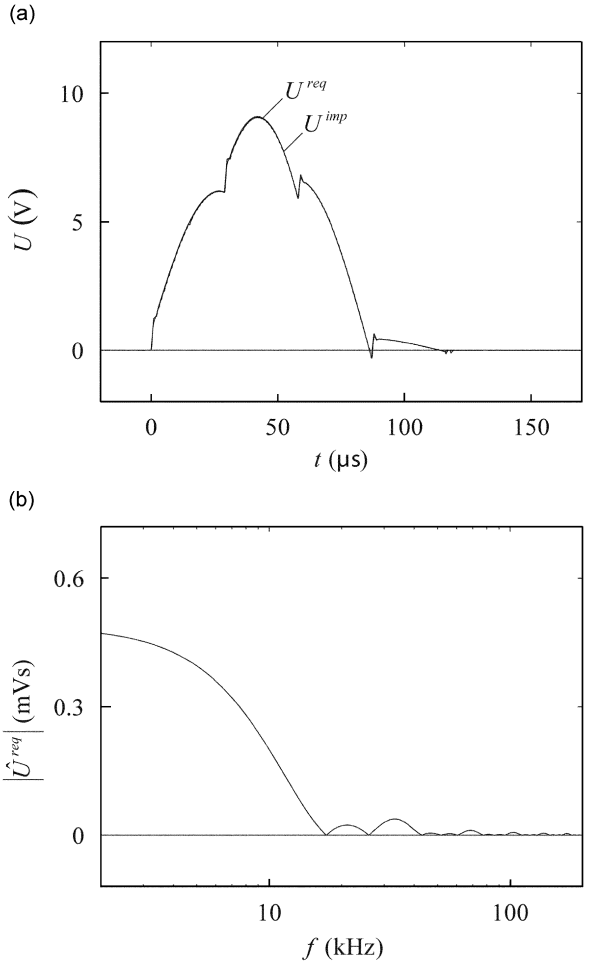

Fig. 11. Generation of single-period sine strain wave: (a) required and implemented input voltages U versus time t and (b) spectrum of required input voltage.

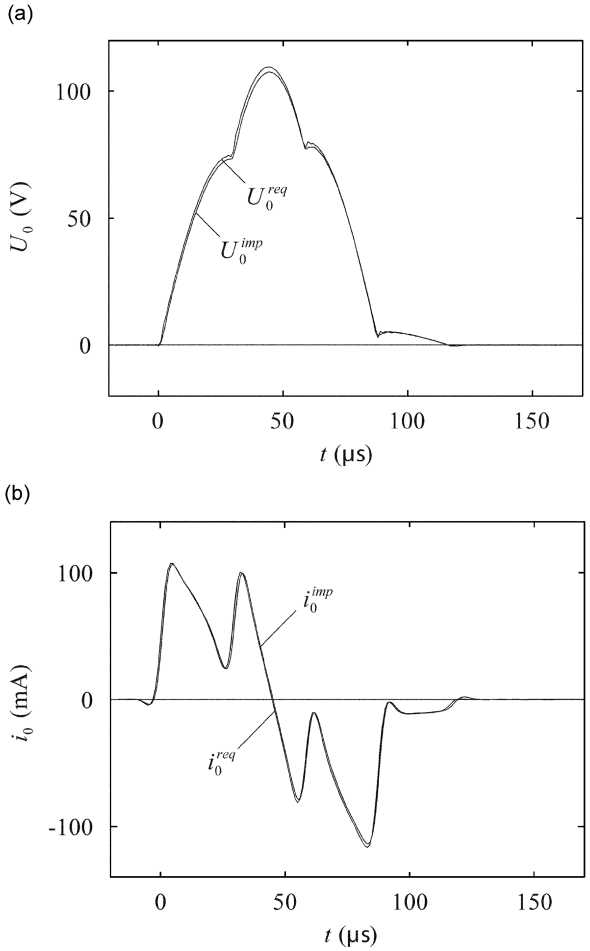

Fig. 12. Generation of single-period sine strain wave. Required and implemented (a) output voltage U_0 and (b) output current i_0 versus time t.

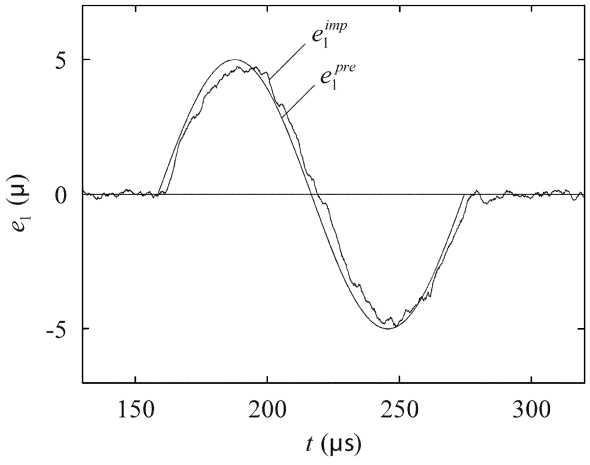

Fig. 13. Generation of single-period sine strain wave. Prescribed and implemented strain e_1 versus time t.

are shown in Fig. 11. The implemented voltage is again very close to that required. The spectrum is significant up to about 50 kHz, which means that the output impedance of the amplifier has little influence. The required and implemented output voltages U_0 and output currents i_0 are shown versus time t in Fig. 12. The implemented voltage and current are again very close to those required. The maximum output current is well below the current limit of 200 mA, which means that the amplifier operated within its linear range. All changes in the input voltage, the output voltage, and the output current again occur in a time approximately equal to the duration $4t_0 \approx 116\,\mu s$ of the prescribed strain pulse. The prescribed and implemented strains e_1 are shown versus time t in Fig. 13. Even though the implemented strain is only 5 μ, it is seen to be insignificantly disturbed by noise, and the agreement with the prescribed strain is good also in this case.

5. Conclusions

The main conclusions of this study are as follows: (i) with the parametric model of the amplifier, the input voltage required for generation of a prescribed strain wave in the bar can be obtained by solving a linear difference equation for the input voltage. (ii) For the amplifier used, the effect of finite cut-off frequency was larger than that of finite output impedance. (iii) For frequencies below 20 kHz, an ideal amplifier model with constant gain and zero output impedance would be highly accurate. Because of its simplicity, such a model is advantageous in control applications where high computational speed is of primary importance. (iv) Very good agreements were obtained between implemented and required input voltages to the amplifier, output voltages from the amplifier, and output currents from the amplifier. (v) Good agreement was obtained between implemented and prescribed strain waves. (vi) The model of the electromechanical system consisting of linear power amplifier and actuator–bar assembly is quite accurate under the conditions of the wave generation tests carried out.

Acknowledgement

The Authors gratefully acknowledge the economical support they have received from the Swedish Research Council (Contract no. 621-2001-2156).

References

[1] G. Gautschi, *Piezoelectric Sensorics*, Springer, Berlin, Heidelberg, 2002.
[2] R. Puers, W. Claes, W. Sansen, M. De Cooman, J. Duyck, I. Naert, Towards the limits in detecting low-level strain with multiple piezo-resistive sensors, *Sensors and Actuators A (Physical)* 85 (2000) 395–401.
[3] J.K. Dürr, R. Honke, M. von Alberti, R. Sippel, Development of an adaptive lightweight mirror for space application, *Smart Materials and Structures* 12 (2003) 1005–1016.
[4] K.K. Tan, S.C. Ng, S.N. Huang, Assisted reproduction system using piezo actuator. *2004 International Conference on Communications, Circuits and Systems (IEEE Cat. No.04EX914)*, part 2, Vol. 2, 2004, pp. 1200–1203.
[5] T. Ikeda, *Fundamentals of Piezoelectricity*, Oxford University Press, New York, 1990.
[6] E.F. Crawley, J. de Luis, Use of piezoelectric actuators as elements of intelligent structures, *AIAA Journal* 25 (10) (1987) 1373–1385.
[7] J. Pan, C.H. Hansen, S.D. Snyder, A study of the response of a simply supported beam to excitation by a piezoelectric actuator, *Journal of Intelligent Material Systems and Structures* 3 (1) (1992) 3–16.
[8] N.W. Hagood, W.H. Chung, A. von Flotow, Modelling of piezoelectric actuator dynamics for active structural control, *Journal of Intelligent Material Systems and Structures* 1 (3) (1990) 327–354.
[9] R.P. Thornburgh, A. Chattopadhyay, Simultaneous modeling of mechanical and electrical response of smart composite structures, *AIAA Journal* 40 (8) (2002) 1603–1610.
[10] R.P. Thornburgh, A. Chattopadhyay, A. Ghoshal, Transient vibration of smart structures using a coupled piezoelectric-mechanical theory, *Journal of Sound and Vibration* 274 (2004) 53–72.
[11] N.W. Hagood, A. von Flotow, Damping of structural vibrations with piezoelectric materials and passive electrical networks, *Journal of Sound and Vibration* 146 (1991) 243–268.
[12] C. Niezrecki, H.H. Cudney, Improving the power consumption characteristics of piezoelectric actuators, *Journal of Intelligent Material Systems and Structures* 5 (1994) 522–529.
[13] D.J. Leo, Energy analysis of piezoelectric-actuated structures driven by linear amplifiers, *Journal of Intelligent Material Systems and Structures* 10 (1) (1999) 36–45.

[14] A. Jansson, B. Lundberg, Piezoelectric generation of extensional waves in a viscoelastic bar by use of a linear power amplifier: theoretical basis, *Journal of Sound and Vibration* 306 (2007) 318–332.
[15] P. Nauclér, B. Lundberg, T. Söderström, A mechanical wave diode: Using feedforward control for one-way transmission of elastic extensional waves. *IEEE Transactions on Control Systems Technology* (2006), in press.
[16] H. Kolsky, *Stress Waves in Solids*, Dover Publications, Inc., New York, 1963.